

Accelerated relaxation in disordered solids under cyclic loading with alternating shear orientation

Nikolai V. Priezjev^{1,2}

¹*Department of Mechanical and Materials Engineering,*

Wright State University, Dayton, OH 45435 and

²*National Research University Higher School of Economics, Moscow 101000, Russia*

(Dated: March 25, 2022)

Abstract

The effect of alternating shear orientation during cyclic loading on the relaxation dynamics in disordered solids is examined using molecular dynamics simulations. The model glass was initially prepared by rapid cooling from the liquid state and then subjected to cyclic shear along a single plane or periodically alternated in two or three dimensions. We showed that with increasing strain amplitude in the elastic range, the system is relocated to deeper energy minima. Remarkably, it was found that each additional alternation of the shear orientation in the deformation protocol brings the glass to lower energy states. The results of mechanical tests after more than a thousand shear cycles indicate that cyclic loading leads to the increase in strength and shear-modulus anisotropy.

Keywords: metallic glasses, periodic deformation, yield stress, molecular dynamics simulations

I. INTRODUCTION

Understanding the response of metallic glasses to mechanical and thermal loading is important for a broad range of applications in biomedical engineering and environmental science [1]. Unlike crystalline materials, where plastic deformation can be described in terms of topological line defects, the amorphous structure of glasses lacks long-range order and can be changed via collective rearrangements of small groups of atoms [2, 3]. During thermomechanical processing, the glasses can be brought to either higher energy, rejuvenated states or to lower energy, relaxed states [4]. The rejuvenated samples are typically less brittle, whereas relaxed glasses exhibit high yield stress and greater chemical stability, among other advantages [4]. There are a number of experimental techniques that can be used to increase the stored energy; namely, high pressure torsion, ion irradiation, wire drawing, and shot peening. Moreover, it was shown that prolonged static loading below the yield stress can induce either irreversible structural rearrangements or the formation of nanocrystals in the metallic glass matrix, leading to improved plasticity [5–11]. Alternatively, aged glasses can be rejuvenated by recovery annealing above the glass transition temperature and then cooled down with a suitably fast rate [12–16]. The mechanical and magnetic properties can also be tuned by repeated thermal cycling at ambient pressure, which might result in rejuvenation or relaxation depending on the system size and thermal amplitude [17–24]. Nevertheless, the combined effect of periodic mechanical deformation and thermal cycling on the extent of relaxation and rejuvenation remains largely unexplored.

In recent years, a number of groups have studied the structural relaxation and dynamical properties of disordered solids under periodic loading using atomistic simulations [25–42]. In particular, it was found that during cyclic shear along a single plane, amorphous systems relocate to lower energy states via a sequence of collective, irreversible rearrangements of atoms when the strain amplitude is below the yielding strain [25–30, 33, 37, 38, 40–42]. In the case of athermal quasistatic loading, the disordered systems eventually reach a special dynamical state, the so-called limit cycle, where the particle dynamics becomes exactly reversible after one or several cycles [26, 27, 29, 33]. At larger strain amplitudes, the yielding transition typically occurs after a number of transient cycles and it is accompanied by the formation of a shear band where the flow is localized and the potential energy is enhanced [33, 34, 38]. More recently, it was shown that shearing along a single or alternating planes did

not result in significant difference of the potential energy when the strain amplitude is close to the critical value [40]. However, despite extensive efforts to access low energy states via mechanical agitation, the development of more efficient deformation protocols remains a challenge.

In this paper, the influence of cyclic deformation with alternating orientation of the shear plane on structural relaxation in binary glasses is investigated via molecular dynamics simulations. We consider a poorly annealed glass at a temperature well below the glass transition temperature and impose periodic shear strain deformation for over a thousand cycles. It will be shown that, in general, glasses relocate to lower energy states with increasing strain amplitude in the elastic range. Moreover, for a given strain amplitude, the relaxation is accelerated when an additional shear orientation is implemented in the deformation protocol. As a result of cyclic loading, the relaxed glasses exhibit an increase in strength and elastic stress anisotropy.

The rest of the paper is divided into three sections. The description of the model, preparation procedure, and deformation protocols is given in the next section. The analysis of the potential energy series and mechanical properties is presented in section III. The last section contains a brief summary.

II. MOLECULAR DYNAMICS (MD) SIMULATIONS

The model glass is represented via the binary (80:20) mixture with strongly non-additive interaction between different types of atoms, which prevents crystallization [43]. The Kob-Andersen (KA) model was extensively studied in the last twenty years and it is often used as a benchmark for testing novel algorithms to examine statistical properties of glassy systems [43]. In this model, the interaction between atoms $\alpha, \beta = A, B$ is described via the Lennard-Jones (LJ) potential:

$$V_{\alpha\beta}(r) = 4\varepsilon_{\alpha\beta} \left[\left(\frac{\sigma_{\alpha\beta}}{r} \right)^{12} - \left(\frac{\sigma_{\alpha\beta}}{r} \right)^6 \right], \quad (1)$$

with the following parametrization: $\varepsilon_{AA} = 1.0$, $\varepsilon_{AB} = 1.5$, $\varepsilon_{BB} = 0.5$, $\sigma_{AA} = 1.0$, $\sigma_{AB} = 0.8$, $\sigma_{BB} = 0.88$, and $m_A = m_B$ [43]. We simulate a relatively large system of 60 000 atoms and use the cutoff radius $r_{c, \alpha\beta} = 2.5 \sigma_{\alpha\beta}$ to reduce the computational efforts. In the following, unless otherwise specified, the MD results are reported in the LJ units of length, mass,

energy, and time: $\sigma = \sigma_{AA}$, $m = m_A$, $\varepsilon = \varepsilon_{AA}$, and $\tau = \sigma\sqrt{m/\varepsilon}$. The simulations were carried out using the LAMMPS parallel code [44] with the time step $\Delta t_{MD} = 0.005\tau$.

The binary mixture was first thoroughly equilibrated at the temperature $T_{LJ} = 1.0\varepsilon/k_B$ and density $\rho = \rho_A + \rho_B = 1.2\sigma^{-3}$. Here, the parameters k_B and T_{LJ} stand for the Boltzmann constant and temperature, respectively. The system temperature was controlled via the Nosé-Hoover thermostat [44, 45]. Note that periodic boundary conditions were imposed along all three spatial dimensions. The corresponding box size at the density $\rho = 1.2\sigma^{-3}$ is $L = 36.84\sigma$. The critical temperature of the KA model at this density is $T_c = 0.435\varepsilon/k_B$ [43]. After equilibration, the system was linearly cooled to the very low temperature $T_{LJ} = 0.01\varepsilon/k_B$ with the fast rate of $10^{-2}\varepsilon/k_B\tau$ at constant volume.

Next, the glass was subjected to periodic shear strain deformation with the oscillation period $T = 5000\tau$ and frequency $\omega = 2\pi/T = 1.26 \times 10^{-3}\tau^{-1}$, as follows:

$$\gamma(t) = \gamma_0 \sin(2\pi t/T), \quad (2)$$

where γ_0 is the strain amplitude. The deformation protocol consists of either periodic shear along the xz plane, or alternating shear along the xz and yz planes, or alternating shear along the xz , yz , and xy planes. In all cases, the sample was deformed during 1400 shear cycles with strain amplitudes, $\gamma_0 \leq 0.065$, in the elastic range at $T_{LJ} = 0.01\varepsilon/k_B$ and $\rho = 1.2\sigma^{-3}$. After cyclic loading, the samples were relaxed during $10^4\tau$ at zero strain and $T_{LJ} = 0.01\varepsilon/k_B$, and then sheared with the rate $10^{-5}\tau^{-1}$ at constant volume along the xz , yz , and xy planes. The shear modulus and the maximum value of the shear stress were computed from the stress-strain response at constant strain rate. In addition, the potential energy, system dimensions, stress components, and atomic configurations were saved for the post-processing analysis. A typical MD simulation of 1400 shear cycles required about 900 hours using 40 processors. Due to computational limitations, the simulations of periodic shear deformation were performed only for one sample.

III. RESULTS

It is well known that in amorphous materials at very low temperatures, the motion of atoms mostly involves vibration within cages formed by their neighbors, and, as a result, the structural relaxation is strongly suppressed. One way to induce collective rearrangements of

atoms and to access lower energy states is to periodically deform the material with the strain amplitude below the yielding point [46]. Under applied strain, the potential energy landscape becomes tilted, and a group of atoms might relocate to a lower energy minimum. A number of recent MD studies have shown that under cyclic shear along a single plane, disordered solids are driven to lower energy states via irreversible rearrangements of atoms [25–27, 30, 33, 37, 38]. Moreover, it was found that athermal systems eventually reach a fully reversible limit cycle and settle down at a particular energy level [26, 27, 29, 33], while in the presence of thermal fluctuations, glasses continue to explore lower energy states, although the size of clusters of mobile atoms becomes progressively smaller [37–39].

The slowing down of the relaxation dynamics during cyclic shear along a single plane implies the existence of the lowest bound in energy that can be attained using such deformation protocol. On the other hand, if the direction of the cyclic shear plane is changed after a number of cycles, then the shear strain in the new direction might allow for larger-scale rearrangements and, consequently, relocation to deeper energy states. It remains an open question whether a fully reversible state with a lower potential energy can be reached in athermal systems using a combination of shear cycles oriented along different directions. In the present study, we compare three deformation protocols where the cyclic shear is either oriented along a single plane or periodically alternated in two and three dimensions. The simulations are performed at strain amplitudes below the yielding transition. It was recently shown using athermal simulations that the critical strain amplitude of the KA mixture at the density $\rho = 1.2 \sigma^{-3}$ is in the range $0.07 < \gamma_0 < 0.08$, and it might depend on the system size, since the nucleation of a shear band is determined by its total interfacial area [26, 33]. In the presence of thermal fluctuations, the critical strain amplitude is reduced with increasing system temperature [25, 37, 38].

The dependence of the potential energy as a function of time during periodic shear along a single plane (xz) is shown in Fig. 1 for the strain amplitudes $\gamma_0 = 0.01, 0.03,$ and 0.06 . Here, the time is expressed in oscillation periods. It can be clearly observed that with increasing strain amplitude, the system relocates to deeper energy minima and the amplitude of potential energy oscillations becomes larger. At lower strain amplitudes, $\gamma_0 = 0.01$ and 0.03 , the potential energy gradually approaches nearly constant levels via occasional sudden drops, which are associated with irreversible rearrangements of groups of atoms. Notice, for

example, the step at $t \approx 580T$ for $\gamma_0 = 0.01$ in Fig. 1. By contrast, the potential energy at $\gamma_0 = 0.06$ is significantly lower and it is subject to large fluctuations, which occur due to the finite temperature and γ_0 being sufficiently close to the critical value. Thus, it was shown that the potential energy minima approach a constant level after about 100 shear cycles at $\gamma_0 = 0.06$, when a poorly annealed glass was periodically deformed using the athermal quasistatic protocol [33].

Next, the effect of alternating shear orientation on the potential energy minima is demonstrated in Fig. 2 for different deformation protocols at the strain amplitude $\gamma_0 = 0.06$. In the case of periodic shear along the xz plane at $\gamma_0 = 0.06$, shown in Fig. 1, only the potential energies at the end of each cycle are replotted in Fig. 2. The other three deformation protocols involve (a) 10 consecutive shear cycles along the xz plane, followed by 10 shear cycles along the yz plane, (b) alternating shear along the xz and yz planes, and (c) alternating shear along the xz , yz , and xy planes. The results in Fig. 2 indicate that each additional alternation of the shear orientation in the deformation protocol leads to lower energy states. In particular, it can be seen that the potential energy minima become significantly lower even when the shear is applied along the same plane for a number of cycles before its orientation is changed (every 10 cycles). Among all protocols, the lowest energy ($U \approx -8.29\varepsilon$) is attained in the limiting case when the orientation of the shear plane is alternated after every cycle in all three spatial dimensions. For comparison, when the KA mixture is cooled with the slow rate $10^{-5}\varepsilon/k_B\tau$ at $\rho = 1.2\sigma^{-3}$, the energy is $U \approx -8.31\varepsilon$ [34].

The summary of the potential energy during 1400 cycles for three different protocols is presented in Fig. 3 for the strain amplitudes in the elastic range $0 \leq \gamma_0 \leq 0.065$. Note that the data for the undeformed glass ($\gamma_0 = 0$) are the same in all three panels in Fig. 3. It can be seen that at the low temperature $T_{LJ} = 0.01\varepsilon/k_B$, the potential energy level for the poorly annealed glass in the absence of deformation remains nearly unchanged during the time interval $1400T$. As indicated in Fig. 3, the deformation procedure includes either periodic shear along one plane or alternating shear along two and three directions. As expected, for each deformation protocol, the system reaches lower energy states when samples are deformed with larger strain amplitudes. Most importantly, it can be observed in Fig. 3 that for each value of γ_0 , the potential energy curves become lower when an additional shear orientation is introduced in the deformation protocol. We further comment that the energy

curves are nearly the same (within fluctuations) for $\gamma_0 = 0.06$ and 0.065 in the panels (b) and (c) in Fig. 3, possibly because the critical strain amplitude for these two protocols is slightly smaller than in the case of periodic shear along the xz plane, shown in Fig. 3 (a).

There are several remarks to be made regarding the influence of temperature and strain amplitude on the potential energy series and the yielding transition. The results of test simulations using three different deformation protocols at the larger strain amplitude $\gamma_0 = 0.07$ have shown that the flow becomes localized typically within the first 300 shear cycles, leading to higher energy levels in steady state (not shown). An accurate estimation of the critical value of the strain amplitude for different deformation protocols is not the main focus of the present study and it might be addressed in the future. An example of the potential energy dependence on time near the critical strain amplitude during cyclic shear along a single plane at $T_{LJ} = 0.1 \varepsilon/k_B$ was reported in Fig. 2 of the previous study [38]. We also comment that the yielding transition was not detected during the first 600 shear cycles with the strain amplitude $\gamma_0 = 0.07$ at the temperature $T_{LJ} = 0.01 \varepsilon/k_B$ [37]. In that study, however, the preparation procedure and the temperature control were different; namely, the dissipative particle dynamics thermostat versus the Nosé-Hoover thermostat, which might lead to delay in the onset of the yielding transition.

The effect of cyclic annealing on mechanical properties was investigated by imposing steady shear with the rate of $10^{-5} \tau^{-1}$ at constant volume and temperature $T_{LJ} = 0.01 \varepsilon/k_B$. Fig. 4 shows the stress-strain curves after aging and cyclic loading with the strain amplitude $\gamma_0 = 0.06$. In each case, after $1400 T$, the samples were relaxed at mechanical equilibrium during $10^4 \tau$ and then steadily strained along the xz , yz , and xy planes in order to examine the stress response and mechanical anisotropy. It can be seen in Fig. 4 (a) that in the absence of cyclic loading, the shear stress remains isotropic and it monotonically increases to a plateau level, as expected for an amorphous material prepared with a relatively fast cooling rate. As is evident from Fig. 4 (b), after cyclic loading along the xz plane, the stress response shows a pronounced yielding peak, and the shear stress σ_{xz} becomes smaller than σ_{yz} and σ_{xy} . In other words, the cyclic loading along a certain plane leads to a reduced stress along that plane compared to the other directions, while the height of the stress overshoot remains insensitive to the shear direction.

The stress-strain curves for the samples that were cyclically deformed with alternating

shear along two and three directions are presented in panels (c) and (d) of Figure 4. In both cases, the shape of the curves remains very similar, although one can notice a slight increase in the height of the yielding peak when the deformation protocol consists of alternating shear along three directions. This is consistent with the lowest energy minimum after 1400 cycles at $\gamma_0 = 0.06$ reported in Fig. 3 (c). It can also be observed in Fig. 4 (c) that the slope of the stress-strain dependence is larger along the xy plane, which was not deformed during cyclic loading. Furthermore, the variation of the shear modulus and yielding peak as a function of the strain amplitude is plotted in Fig. 5. The data are somewhat scattered but the general conclusions can be formulated as follows. First, the height of the yielding peak increases when an additional shear orientation is introduced in the cyclic loading protocol. Second, the shear modulus is larger along the shear directions that were not used during the cyclic deformation.

We next discuss the analysis of nonaffine displacements during shear deformation and provide a visual comparison of strained samples that were prepared with different cyclic loading protocols. By definition, the nonaffine displacement of an atom i with respect to its neighbors can be computed using the matrix \mathbf{J}_i , which linearly transforms the group of neighboring atoms during the time interval Δt and minimizes the following expression:

$$D^2(t, \Delta t) = \frac{1}{N_i} \sum_{j=1}^{N_i} \left\{ \mathbf{r}_j(t + \Delta t) - \mathbf{r}_i(t + \Delta t) - \mathbf{J}_i [\mathbf{r}_j(t) - \mathbf{r}_i(t)] \right\}^2, \quad (3)$$

where the sum is over the nearest-neighbors within the distance of 1.5σ from the location of the i -th atom at $\mathbf{r}_i(t)$. It was originally shown that the local shear transformations in disordered solids can be accurately identified using a sufficiently large threshold value of the nonaffine measure [47]. More recently, it was found that during cyclic deformation of amorphous alloys, the typical size of clusters of atoms with large nonaffine displacements becomes progressively smaller when the strain amplitude is below the yielding point [37–39]. By contrast, the yielding transition in both poorly and well annealed glasses at a finite temperature is associated with the formation of a system-spanning shear band after a number of transient cycles [34, 38].

The representative examples of the spatial evolution of nonaffine displacements are illustrated in Figs. 6-9 for selected stress-strain curves shown in Fig. 4. In all cases, the nonaffine measure is computed with respect to zero strain and indicated by the color according to the

legend. As shown in Fig. 6, the plastic deformation of the aged sample is initially rather homogeneous, and the flow becomes localized only when $\gamma_{xz} = 0.20$. In contrast, after cyclic loading along the xz plane, the nucleation of the shear band is apparent right after the yielding peak at $\gamma_{yz} = 0.10$ and it becomes wider with increasing strain, as shown in Fig. 7. Note that in this case the glass is strained along the yz plane, which is perpendicular to the plane of cyclic shear. Similar patterns are evident in strained samples that were cyclically loaded with alternating shear along two (see Fig. 8) and three (see Fig. 9) directions. Altogether, these results indicate that cyclic loading within the elastic regime leads to the increase in strength and pronounced shear localization.

IV. CONCLUSIONS

In summary, a comparison of different cyclic deformation protocols aiming to access more relaxed states in disordered solids was performed using molecular dynamics simulations. We considered a model glass represented by a strongly non-additive binary mixture, which was first rapidly cooled from the liquid state to a very low temperature and then subjected to cyclic loading within the elastic regime. The deformation protocols include cyclic shear either along a single plane or periodically alternated along two or three mutually perpendicular planes. Our main conclusion is that an additional orientation of the shear plane during the oscillatory shear deformation results in more relaxed states, provided that the strain amplitude is smaller than the yield strain. Thus, the lowest potential energy level is attained in the case of alternating orientation of the shear plane along all three spatial dimensions. After cyclic loading, the mechanical properties were probed in relaxed samples steadily strained along different directions. Interestingly, the shear modulus tends to be larger along the shear planes that were not used in the cyclic deformation protocol. The analysis of the stress response indicated that the peak height of the stress overshoot increases in glasses cycled with larger strain amplitudes.

Acknowledgments

Financial support from the National Science Foundation (CNS-1531923) is gratefully acknowledged. The author would like to thank C. Reichhardt for drawing attention to the

problem of cyclic loading with alternating shear orientation. The article was prepared within the framework of the HSE University Basic Research Program and funded in part by the Russian Academic Excellence Project ‘5-100’. The numerical simulations were performed at Wright State University’s Computing Facility and the Ohio Supercomputer Center. The molecular dynamics simulations were carried out using the LAMMPS software developed at Sandia National Laboratories [44].

- [1] B. Ruta, E. Pineda, and Z. Evenson, Relaxation processes and physical aging in metallic glasses, *J. Phys. Condens. Matter* **29**, 503002 (2017).
- [2] F. Spaepen, A microscopic mechanism for steady state inhomogeneous flow in metallic glasses, *Acta Metall.* **25**, 407 (1977).
- [3] A. S. Argon, Plastic deformation in metallic glasses, *Acta Metall.* **27**, 47 (1979).
- [4] Y. Sun, A. Concustell, and A. L. Greer, Thermomechanical processing of metallic glasses: Extending the range of the glassy state, *Nat. Rev. Mater.* **1**, 16039 (2016).
- [5] K.-W. Park, C.-M. Lee, M. Wakeda, Y. Shibutani, M. L. Falk, and J.-C. Lee, Elastostatically induced structural disordering in amorphous alloys, *Acta Materialia* **56**, 5440 (2008).
- [6] Y. Zhang, N. Mattern, J. Eckert, Effect of uniaxial loading on the structural anisotropy and the dynamics of atoms of $\text{Cu}_{50}\text{Zr}_{50}$ metallic glasses within the elastic regime studied by molecular dynamics simulation, *Acta Materialia* **59**, 4303 (2011).
- [7] Y. Tong, W. Dmowski, Y. Yokoyama, G. Wang, P. K. Liaw, and T. Egami, Recovering compressive plasticity of bulk metallic glasses by high-temperature creep, *Scripta Materialia* **69** 570 (2013).
- [8] J. Gu, M. Song, S. Ni, X. Liao, and S. Guo, Improving the plasticity of bulk metallic glasses via pre-compression below the yield stress, *Mater. Sci. Eng., A* **602**, 68 (2014).
- [9] A. L. Greer, and Y. H. Sun, Stored energy in metallic glasses due to strains within the elastic limit, *Philos. Mag.* **96**, 1643 (2016).
- [10] J. Pan, Y. X. Wang, Q. Guo, D. Zhang, A. L. Greer, and Y. Li, Extreme rejuvenation and softening in a bulk metallic glass, *Nat. Commun.* **9**, 560 (2018).
- [11] N. V. Priezjev, Aging and rejuvenation during elastostatic loading of amorphous alloys: A molecular dynamics simulation study, *Comput. Mater. Sci.* **168**, 125 (2019).

- [12] J. Saida, R. Yamada, and M. Wakeda, Recovery of less relaxed state in Zr-Al-Ni-Cu bulk metallic glass annealed above glass transition temperature, *Appl. Phys. Lett.* **103**, 221910 (2013).
- [13] M. Wakeda, J. Saida, J. Li, and S. Ogata, Controlled rejuvenation of amorphous metals with thermal processing, *Sci. Rep.* **5**, 10545 (2015).
- [14] S. Kuchemann, P. M. Derlet, C. Liu, D. Rosenthal, G. Sparks, W. S. Larson, and R. Maass, Energy Storage in Metallic Glasses via Flash Annealing, *Adv. Funct. Mater.* **28**, 1805385 (2018).
- [15] M. Wang, H. Liu, J. Mo, Y. Zhang, Z. Chen, C. Yin, and W. Yang, Thermal-pressure effects on energy state of metallic glass $\text{Cu}_{50}\text{Zr}_{50}$, *Comput. Mater. Sci.* **155**, 493 (2018).
- [16] N. V. Priezjev, Atomistic modeling of heat treatment processes for tuning the mechanical properties of disordered solids, *J. Non-Cryst. Solids* **518**, 128 (2019).
- [17] S. V. Ketov, Y. H. Sun, S. Nachum, Z. Lu, A. Checchi, A. R. Beraldin, H. Y. Bai, W. H. Wang, D. V. Louzguine-Luzgin, M. A. Carpenter, and A. L. Greer, Rejuvenation of metallic glasses by non-affine thermal strain, *Nature* **524**, 200 (2015).
- [18] F. Bu, J. Wang, L. Li, H. Kou, X. Xue, J. Li, The effect of thermal cycling treatments on the thermal stability and mechanical properties of a Ti-based bulk metallic glass composite, *Metals* **6**, 274 (2016).
- [19] M.-C. Ri, S. Sohrabi, D.-W. Ding, B.-S. Dong, S.-X. Zhou, and W.-H. Wang, Serrated magnetic properties in metallic glass by thermal cycle, *Chin. Phys. B* **26**, 066101 (2017).
- [20] W.-H. Liu, B. A. Sun, H. Gleiter, S. Lan, Y. Tong, X.-L. Wang, H. Hahn, Y. Yang, J.-J. Kai, and C. T. Liu, Nanoscale Structural Evolution and Anomalous Mechanical Response of Nanoglasses by Cryogenic Thermal Cycling, *Nano Lett.* **18**, 4188 (2018).
- [21] N. V. Priezjev, The effect of cryogenic thermal cycling on aging, rejuvenation, and mechanical properties of metallic glasses, *J. Non-Cryst. Solids* **503**, 131 (2019).
- [22] Q.-L. Liu and N. V. Priezjev, The influence of complex thermal treatment on mechanical properties of amorphous materials, *Comput. Mater. Sci.* **161**, 93 (2019).
- [23] N. V. Priezjev, Potential energy states and mechanical properties of thermally cycled binary glasses, *J. Mater. Res.* **34**, 2664 (2019).
- [24] B. S. Li, S. Xie, and J. J. Kruzic, Toughness enhancement and heterogeneous softening of a cryogenically cycled Zr-Cu-Ni-Al-Nb bulk metallic glass, *Acta Materialia* **176**, 278 (2019).

- [25] N. V. Priezjev, Heterogeneous relaxation dynamics in amorphous materials under cyclic loading, *Phys. Rev. E* **87**, 052302 (2013).
- [26] D. Fiocco, G. Foffi, and S. Sastry, Oscillatory athermal quasistatic deformation of a model glass, *Phys. Rev. E* **88**, 020301(R) (2013).
- [27] I. Regev, T. Lookman, and C. Reichhardt, Onset of irreversibility and chaos in amorphous solids under periodic shear, *Phys. Rev. E* **88**, 062401 (2013).
- [28] N. V. Priezjev, Dynamical heterogeneity in periodically deformed polymer glasses, *Phys. Rev. E* **89**, 012601 (2014).
- [29] I. Regev, J. Weber, C. Reichhardt, K. A. Dahmen, and T. Lookman, Reversibility and criticality in amorphous solids, *Nat. Commun.* **6**, 8805 (2015).
- [30] N. V. Priezjev, Reversible plastic events during oscillatory deformation of amorphous solids, *Phys. Rev. E* **93**, 013001 (2016).
- [31] T. Kawasaki and L. Berthier, Macroscopic yielding in jammed solids is accompanied by a non-equilibrium first-order transition in particle trajectories, *Phys. Rev. E* **94**, 022615 (2016).
- [32] N. V. Priezjev, Nonaffine rearrangements of atoms in deformed and quiescent binary glasses, *Phys. Rev. E* **94**, 023004 (2016).
- [33] P. Leishangthem, A. D. S. Parmar, and S. Sastry, The yielding transition in amorphous solids under oscillatory shear deformation, *Nat. Commun.* **8**, 14653 (2017).
- [34] N. V. Priezjev, Collective nonaffine displacements in amorphous materials during large-amplitude oscillatory shear, *Phys. Rev. E* **95**, 023002 (2017).
- [35] M. Fan, M. Wang, K. Zhang, Y. Liu, J. Schroers, M. D. Shattuck, and C. S. O'Hern, The effects of cooling rate on particle rearrangement statistics: Rapidly cooled glasses are more ductile and less reversible, *Phys. Rev. E* **95**, 022611 (2017).
- [36] S. Dagois-Bohy, E. Somfai, B. P. Tighe, and M. van Hecke, Softening and yielding of soft glassy materials, *Soft Matter* **13**, 9036 (2017).
- [37] N. V. Priezjev, Molecular dynamics simulations of the mechanical annealing process in metallic glasses: Effects of strain amplitude and temperature, *J. Non-Cryst. Solids* **479**, 42 (2018).
- [38] N. V. Priezjev, The yielding transition in periodically sheared binary glasses at finite temperature, *Comput. Mater. Sci.* **150**, 162 (2018).
- [39] N. V. Priezjev, Slow relaxation dynamics in binary glasses during stress-controlled, tension-compression cyclic loading, *Comput. Mater. Sci.* **153**, 235 (2018).

- [40] P. Das, A. D. S. Parmar, and S. Sastry, Annealing glasses by cyclic shear deformation, arXiv:1805.12476 (2018).
- [41] N. V. Priezjev and M. A. Makeev, The influence of periodic shear on structural relaxation and pore redistribution in binary glasses, *J. Non-Cryst. Solids* **506**, 14 (2019).
- [42] N. V. Priezjev and M. A. Makeev, Structural transformations during periodic deformation of low-porosity amorphous materials, *Modelling Simul. Mater. Sci. Eng.* **27**, 025004 (2019).
- [43] W. Kob and H. C. Andersen, Testing mode-coupling theory for a supercooled binary Lennard-Jones mixture: The van Hove correlation function, *Phys. Rev. E* **51**, 4626 (1995).
- [44] S. J. Plimpton, Fast parallel algorithms for short-range molecular dynamics, *J. Comp. Phys.* **117**, 1 (1995).
- [45] M. P. Allen and D. J. Tildesley, *Computer Simulation of Liquids* (Clarendon, Oxford, 1987).
- [46] D. J. Lacks and M. J. Osborne, Energy landscape picture of overaging and rejuvenation in a sheared glass, *Phys. Rev. Lett.* **93**, 255501 (2004).
- [47] M. L. Falk and J. S. Langer, Dynamics of viscoplastic deformation in amorphous solids, *Phys. Rev. E* **57**, 7192 (1998).

Figures

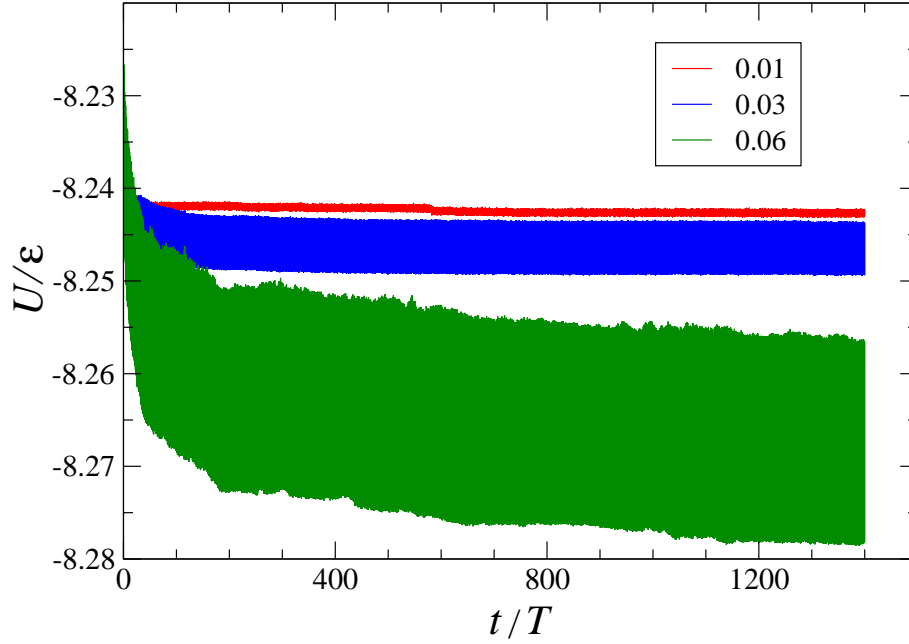


FIG. 1: (Color online) The potential energy series during 1400 shear cycles along the xz plane. The strain amplitudes are $\gamma_0 = 0.01, 0.03,$ and 0.06 (from top to bottom). The period of oscillation is $T = 5000 \tau$.

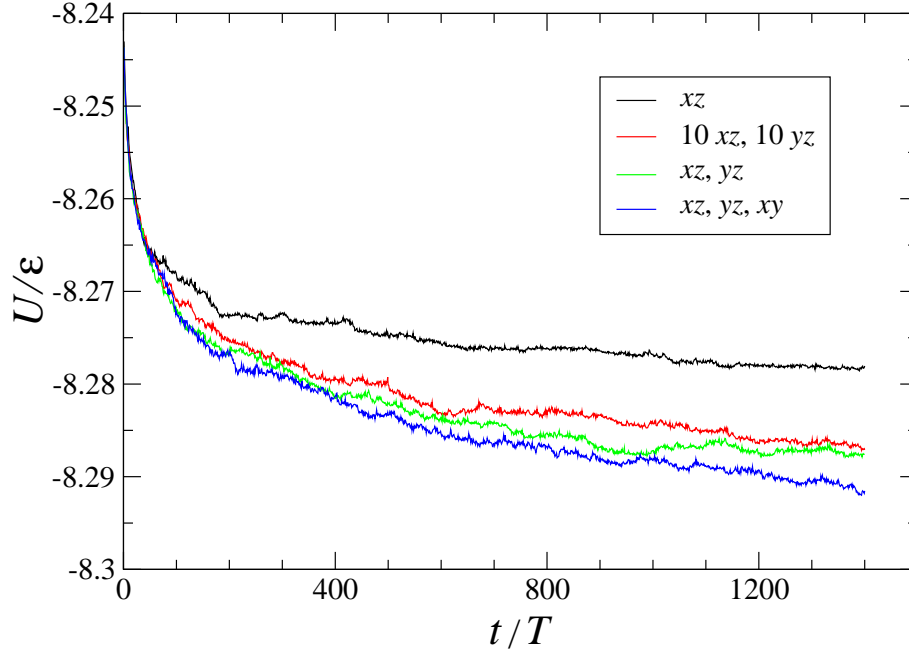


FIG. 2: (Color online) The potential energy minima during 1400 shear cycles for the strain amplitude $\gamma_0 = 0.06$. The deformation protocols include: (1) periodic shear along the xz plane, (2) 10 shear cycles along the xz plane, followed by 10 shear cycles along the yz plane, (3) alternating shear along the xz and yz planes, and (4) alternating shear along the xz , yz , and xy planes, as indicated in the legend. The oscillation period is $T = 5000\tau$ and the temperature is $T_{LJ} = 0.01 \varepsilon/k_B$.

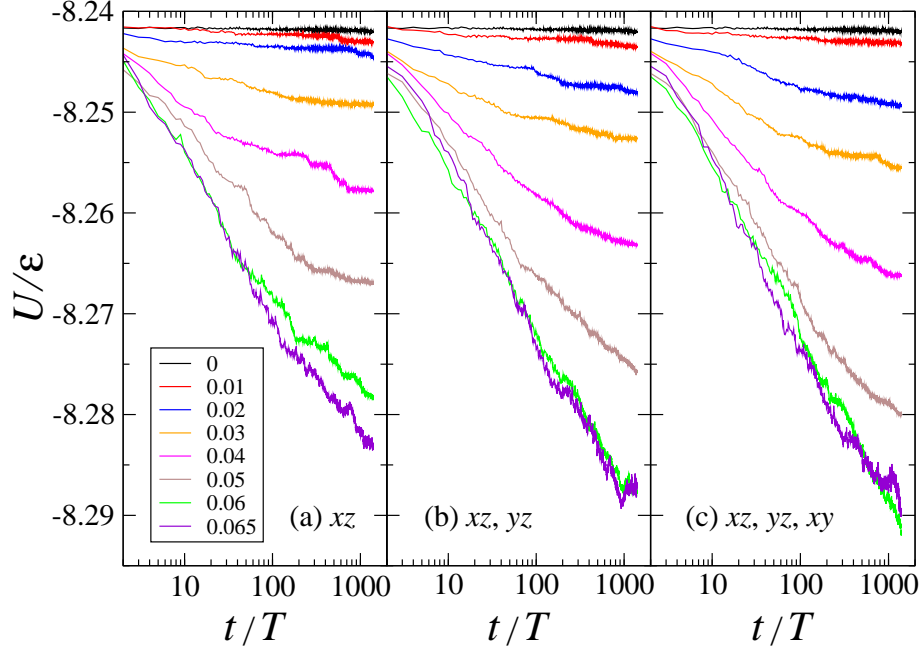


FIG. 3: (Color online) The potential energy at the end of each shear cycle for the indicated strain amplitudes. The deformation is (a) periodic shear along the xz plane, (b) alternating shear along the xz and yz planes, and (c) alternating shear along the xz , yz , and xy planes. The period is $T = 5000 \tau$.

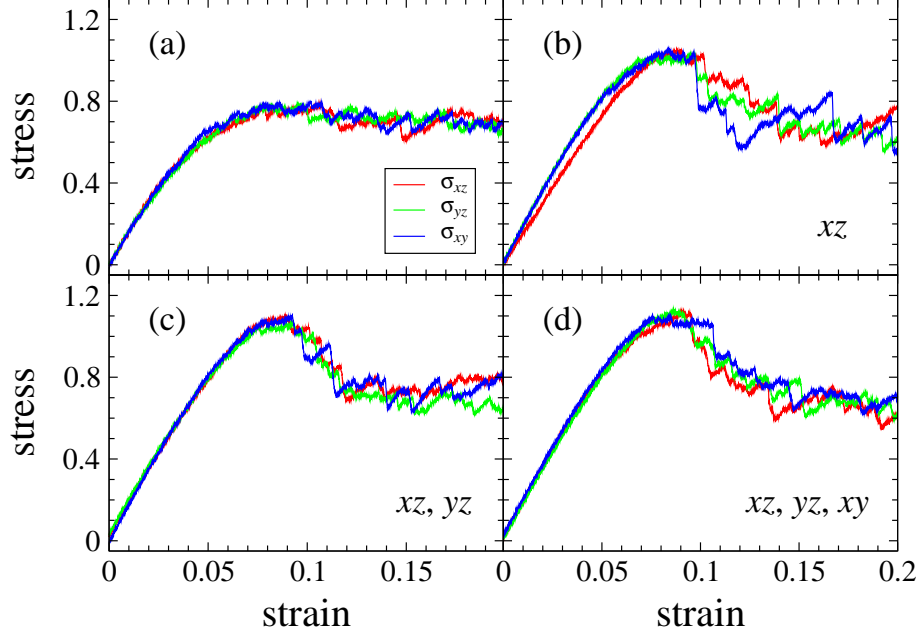


FIG. 4: (Color online) The shear stress (in units of $\varepsilon\sigma^{-3}$) as a function of strain during steady shear with the rate $\dot{\gamma} = 10^{-5} \tau^{-1}$. The plane of shear is parallel to the xz plane (red), the yz plane (green), and the xy plane (blue). The samples were (a) at mechanical equilibrium during 1400T, (b) periodically sheared along the xz plane, (c) sheared along the xz and yz planes, and (d) deformed along the xz , yz , and xy planes. See text for details.

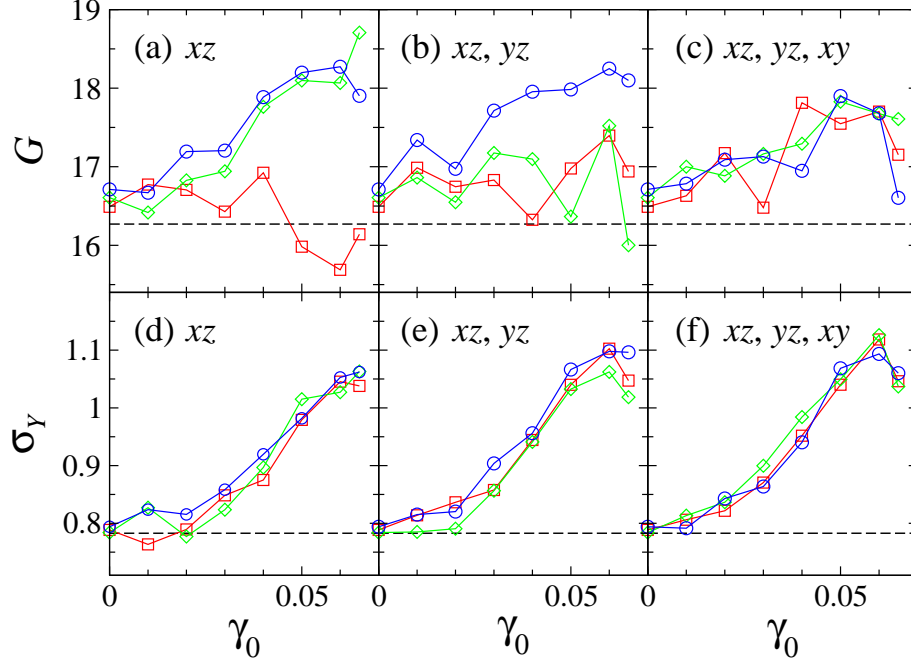


FIG. 5: (Color online) The shear modulus G (in units of $\varepsilon\sigma^{-3}$, upper panels) and the yielding peak σ_Y (in units of $\varepsilon\sigma^{-3}$, lower panels) measured after 1400 shear cycles with the strain amplitude γ_0 . The annealing protocols include: (a, d) periodic shear along the xz plane, (b, e) alternating shear along the xz and yz planes, and (c, f) alternating shear along the xz , yz , and xy planes. Both G and σ_Y are computed from the stress-strain curves during steady shear along the xz plane (\square), along the yz plane (\diamond), and along the xy plane (\circ). The horizontal dashed lines denote the data before periodic loading.

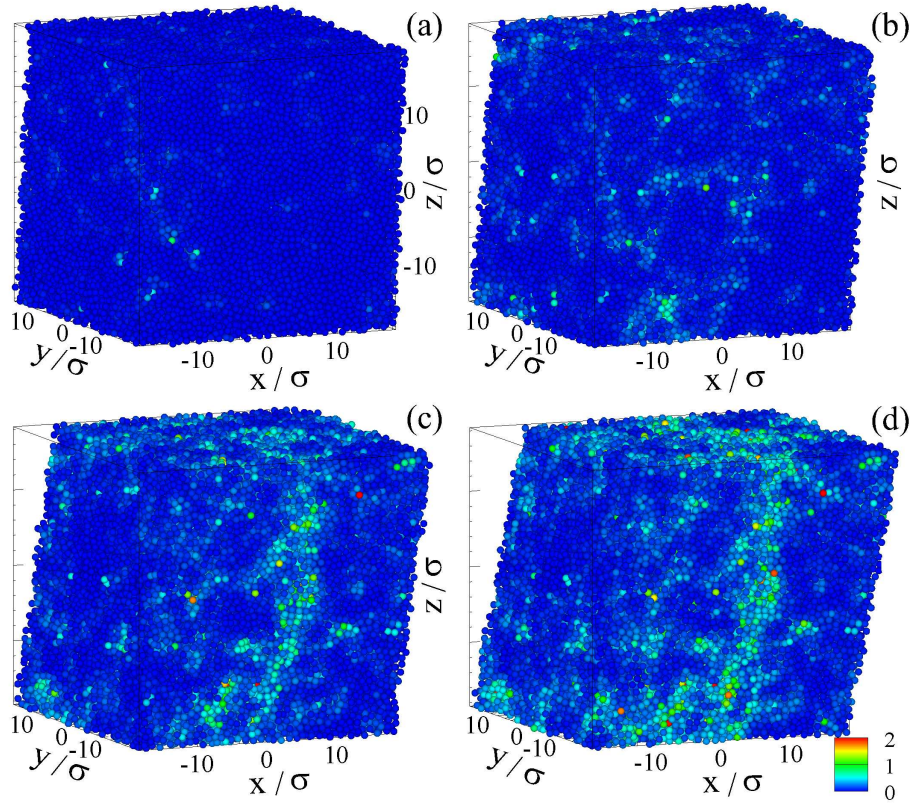


FIG. 6: (Color online) The sequence of snapshots for the glass aged during $1400T$ at $T_{LJ} = 0.01 \varepsilon/k_B$ and then strained along the xz plane. The strain rate is $10^{-5} \tau^{-1}$ and the shear strain is (a) 0.05, (b) 0.10, (c) 0.15, and (d) 0.20. The color indicates the value of the nonaffine measure with respect to $\gamma_{xz} = 0$, according to the legend.

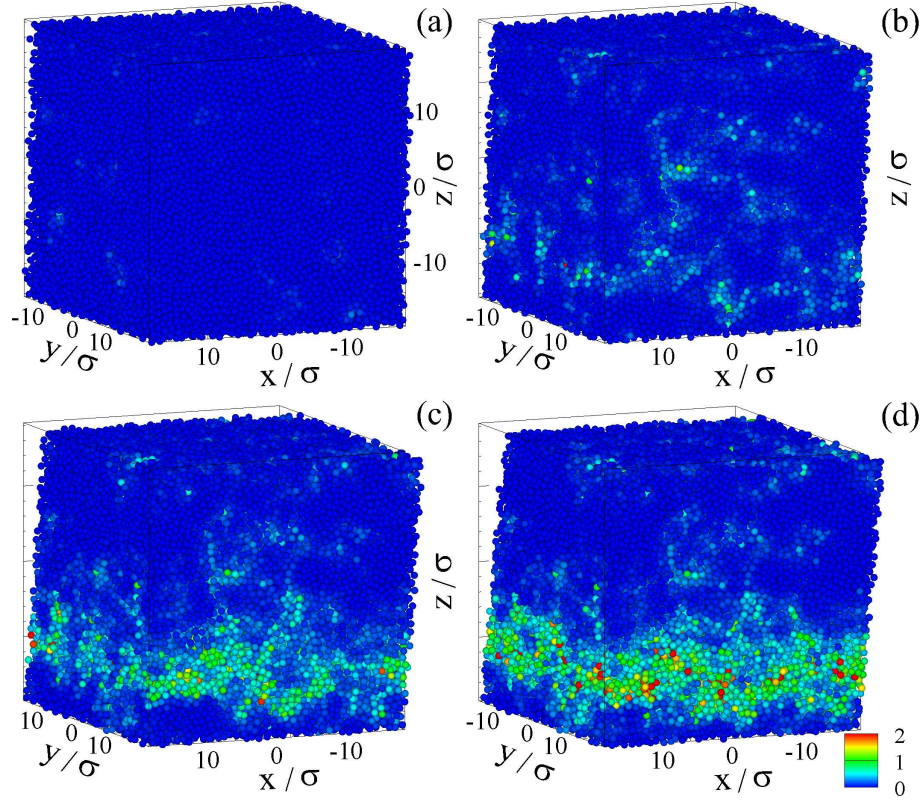


FIG. 7: (Color online) Instantaneous atomic configurations at the shear strain (a) $\gamma_{yz} = 0.05$, (b) $\gamma_{yz} = 0.10$, (c) $\gamma_{yz} = 0.15$, and (d) $\gamma_{yz} = 0.20$. The sample was initially deformed during 1400 shear cycles along the xz plane. The color denotes D^2 with respect to zero strain.

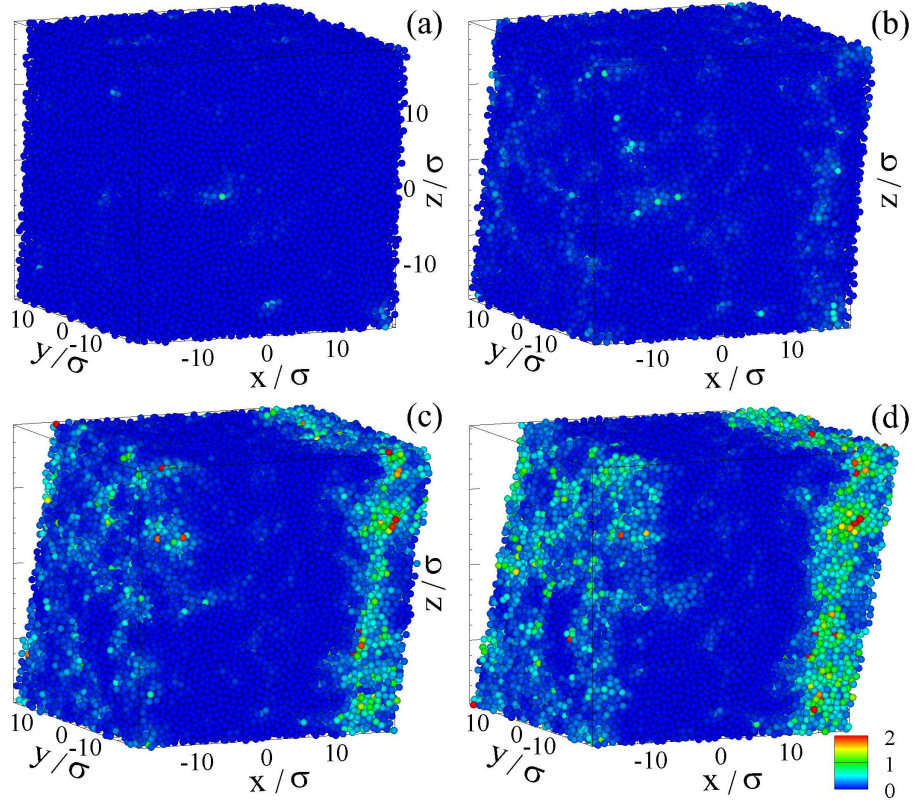


FIG. 8: (Color online) A series of snapshots during steady shear along the xz plane with the rate of $10^{-5} \tau^{-1}$. The shear strain is (a) $\gamma_{xz} = 0.05$, (b) 0.10, (c) 0.15, and (d) 0.20. The shear strain was induced after 1400 alternating shear cycles along the xz and yz planes. The nonaffine measure D^2 is indicated according to the legend.

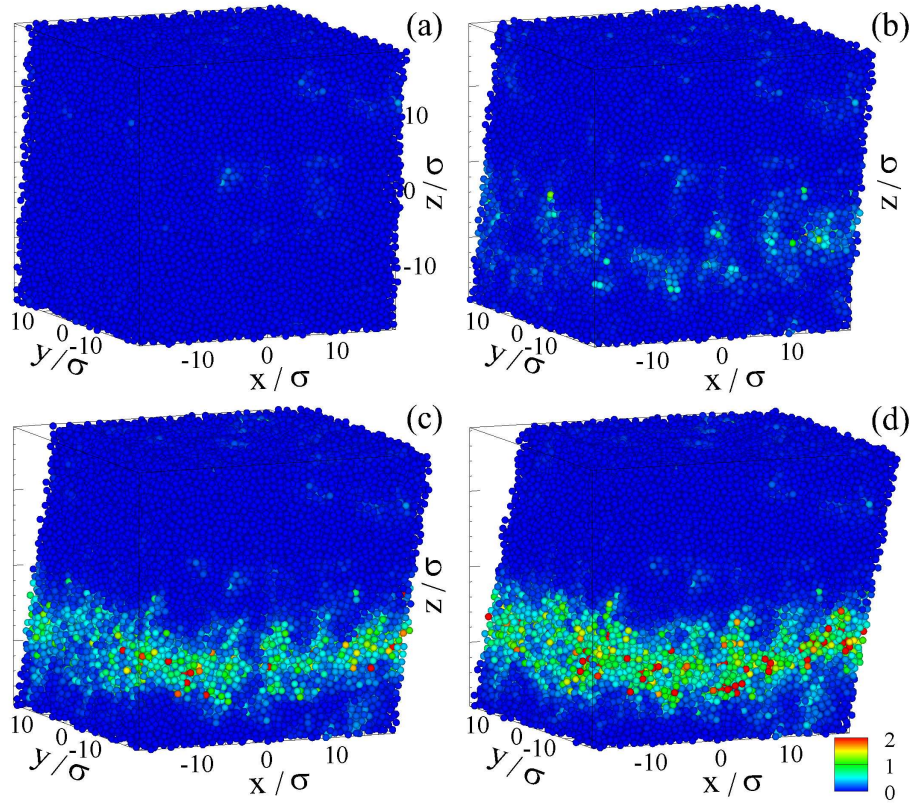


FIG. 9: (Color online) Four snapshots of the strained glass along the xz plane with the rate $10^{-5} \tau^{-1}$. The strain is (a) $\gamma_{xz} = 0.05$, (b) 0.10, (c) 0.15, and (d) 0.20. The annealing protocol consists of alternating shear along the xz , yz , and xy planes. The color code for D^2 is indicated in the legend box.